Journal of Materials Chemistry A

PAPER

View Article Online
View Journal | View Issue

Cite this: J. Mater. Chem. A, 2014, 2, 8026

Isoindigo-based copolymers for polymer solar cells with efficiency over 7%†

Chun-Chih Ho,[a] Chien-An Chen,[b] Chun-Yu Chang,[a] Seth B. Darling[cd] and Wei-Fang Su*[ab]

Received 3rd March 2014
Accepted 11th March 2014

DOI: 10.1039/c4ta01083c

www.rsc.org/MaterialsA

A series of isoindigo-based low-band-gap copolymers (P*n*TI) containing an extended thiophene unit in the donor segment of the polymer were synthesized. The results show that the extended thiophene unit with centrosymmetric conformation simultaneously broadens the polymer absorption and enhances the crystallinity and, thus, hole mobility. Consequently, with additional improved solubility, the polymer **P6TI** exhibits the highest PCE of 7.25% (and a high J_{sc} of 16.24 mA cm^{-2}) among isoindigo-based low-band-gap copolymers. This work demonstrates that by simply adjusting the donor segment and with relatively simple synthetic schemes, a material for high-performance and scalable PSCs will become available.

Introduction

Polymer solar cells (PSCs) have recently drawn intense focus as an alternative to inorganic photovoltaic devices due to their advantages of light weight, flexibility, and facile large-scale fabrication.[1–5] The active layer of PSCs with high performance is generally composed of a bulk heterojunction (BHJ) configuration and fabricated from a blended electron-donor (conducting polymer) and electron-acceptor (fullerene derivative).[6–8] In order to obtain a high-efficiency BHJ solar cell, numerous chemical and structural parameters (*e.g.*, conjugated backbone and side chains) must be rationally designed and then adjusted.[9] In particular, the donor–acceptor (D–A) concept is widely utilized to design the main chain of conjugated polymers for PSCs. Through this strategy, the frontier molecular orbital energy levels of the resulting alternating conjugated copolymer can be fine-tuned *via* intramolecular charge transfer (ICT), which leads to a narrow band gap. However, a spectrum comprised of dual-band absorption with poor harvesting in the 400–600 nm range is usually obtained, thereby sacrificing a key portion of absorption from sunlight. In 2010, the Reynolds group described the intramolecular donor–acceptor interactions for spectral engineering, suggesting that the full solar spectrum can be approached through adjusting the composition of donor and acceptor moieties.[10] Although a vast array of D–A low-band-gap polymers have been developed,[11] there are scant few sustainable low-band-gap polymers with wide-range absorption.

Isoindigo as an acceptor moiety has recently attracted attention due to both its strong electron-withdrawing ability contributed from its two lactam rings and the fact that it is a sustainable material extractable from plants.[12,13] Since Reynolds' group first synthesized isoindigo-based small molecules exhibiting favorable absorption spectra and well matched energy levels with PCBM acceptors for photovoltaic (PV) application,[14] researchers have devoted a great deal of effort to develop isoindigo-based molecular and macromolecular materials.[15–32] However, most of these systems exhibit moderate PV performance, and only three polymers have exceeded the power conversion efficiency (PCE) of 6%; one polymer (PiITVT) developed by Jo's group copolymerizes isoindigo with thienylvinylene to strengthen the intermolecular interaction with a better coplanar structure,[31] a second (PBDT-TID) developed by Tan's group[23] attaches the isoindigo moiety on the side chain as an absorber to broaden the light harvesting range, and the third (**P3TI**) developed by Andersson's group[24] and Wang's group[30] copolymerizes isoindigo with terthiophene to enhance the absorption intensity in the high-energy band and have a combination of a favorable morphology and an optimal interfacial energy level offset. In addition, Pei's group[33] reported that the charge carrier mobility of IIDDT (0.79 cm^2 V^{-1} s^{-1}), in which isoindigo is copolymerized with bithiophene, is nearly one order of magnitude higher than that of IIDT, in which isoindigo is copolymerized with monothiophene. The grazing incidence X-ray diffraction (GIXD) pattern reveals edge-on diffraction peaks of the IIDDT up to the fourth order, indicating that this

[a]*Department of Materials Science and Engineering, National Taiwan University, Taipei 106-17, Taiwan. E-mail: suwf@ntu.edu.tw; Tel: +886-3366-4078*

[b]*Institute of Polymer Science and Engineering, National Taiwan University, Taipei, 10617, Taiwan*

[c]*Center for Nanoscale Materials, Argonne National Laboratory, 9700 South Cass Avenue, Lemont, Illinois 60439, USA*

[d]*Institute for Molecular Engineering, University of Chicago, Chicago, Illinois 60637, USA*

† Electronic supplementary information (ESI) available: Experimental procedures, UV-Vis absorption data of polymers, synthesis of monomers and polymers, UV-Vis absorption of blend films, and 1D GIWAXS of polymer films. See DOI: 10.1039/c4ta01083c

polymer can have excellent molecular organization with the assistance of the bithiophene moiety incorporated into the main chain. The broadened absorption range, the increased absorption intensity, and the increased air-stable mobility from these pioneering studies inspired us to modify their chemical structures to intentionally enhance J_{sc} by combining the existing merits and thus the overall PV performance.

Hence, we have synthesized a series of isoindigo-based low-band-gap copolymers, **P3TI**, **P4TI**, **P5TI**, and **P6TI**, simultaneously extending the thiophene moiety and incorporating monothiophene or bithiophene into the donor segment. Notably, recent parallel work from Wang's group[30] discussed another set of P*n*TI polymers and reported that their **P3TI** polymer has the highest PCE of 6.9% due to the combination of favorable morphology and an optimal interfacial energy level offset to ensure efficient exciton separation and charge generation. However, after optimizing the processing conditions, our polymers show promising PV properties with moderate to high PCEs and provide different perspectives from chemical structures. In particular, **P6TI** displays the highest PCE of ~7.25% and J_{sc} of 16.24 mA cm^{-2} among the published isoindigo-based copolymers.

Results and discussion

The synthetic routes to compound **1** to the corresponding polymers are illustrated in Scheme 1, and others not shown here are described in the ESI.† Similar to Andersson *et al.*'s work,[24] octyl was substituted on the thiophene units to ensure enough solubility; all octyl substituents were designed to face the center of donor segments to improve the planarity of the polymer main chain and lessen steric hindrance from the side chain of the isoindigo unit.[34] Compound **1** and trimethyl(4-octylthiophen-2-yl) were prepared using a modified procedure according to the previous work.[24] These two compounds were coupled by the Stille coupling reaction to yield compound **2** with high yield (>97%). Compound **2** was then reacted with *N*-bromosuccinimide (NBS) for the bromination to provide compound **3** (89% yield). The obtained compound **1** and compound **3** were respectively copolymerized with commercially available 2,5-bis(trimethylstannyl)thiophene or 5,5′-bis(trimethylstannyl)-2,2′-bithiophene *via* the microwave-assisted Stille coupling reaction to afford **P3TI**, **P4TI**, **P5TI**, and **P6TI** (>72% yield). These polymers were purified by Soxhlet extraction in a sequence of methanol, acetone, and hexane (additional THF for **P4TI** and **P6TI**) to remove the low molecular weight impurity and then filtered through Celite to remove the catalyst residue.[35] The number-average molecular weight (M_n) and molecular weight distribution (PDI) of the polymers were determined by high-temperature gel permeation chromatography (HT-GPC) at 135 °C using 1,2,4-trichlorobenzene as the eluent and monodisperse polystyrene as the calibration standard, and are in the range of 25k–50k and 1.8–2.5, respectively (Table 1). The GPC traces of all polymers are shown in the ESI.† The polymers can be dissolved in common organic solvents such as chloroform (CF), chlorobenzene (CB), and *o*-dichlorobenzene (DCB). Note, although two additional octyl groups are substituted on the thiophene units of **P4TI** as compared to P2TI reported by Pei's group,[36] its solubility is not as good as other polymers.

The UV-Vis absorption spectra of all polymers in chloroform solution and as-cast thin films are shown in Fig. 1, and their optical properties are listed in Table 1. As expected, all polymers show two evident absorption bands and increased intensity of the high-energy band with extending the donor segment in both the solutions and films. The increased intensity is proportional to the number of thiophene units because the high-energy absorption band is usually attributed to the π–π* transition from the donor segments. For solutions, the low-energy bands,

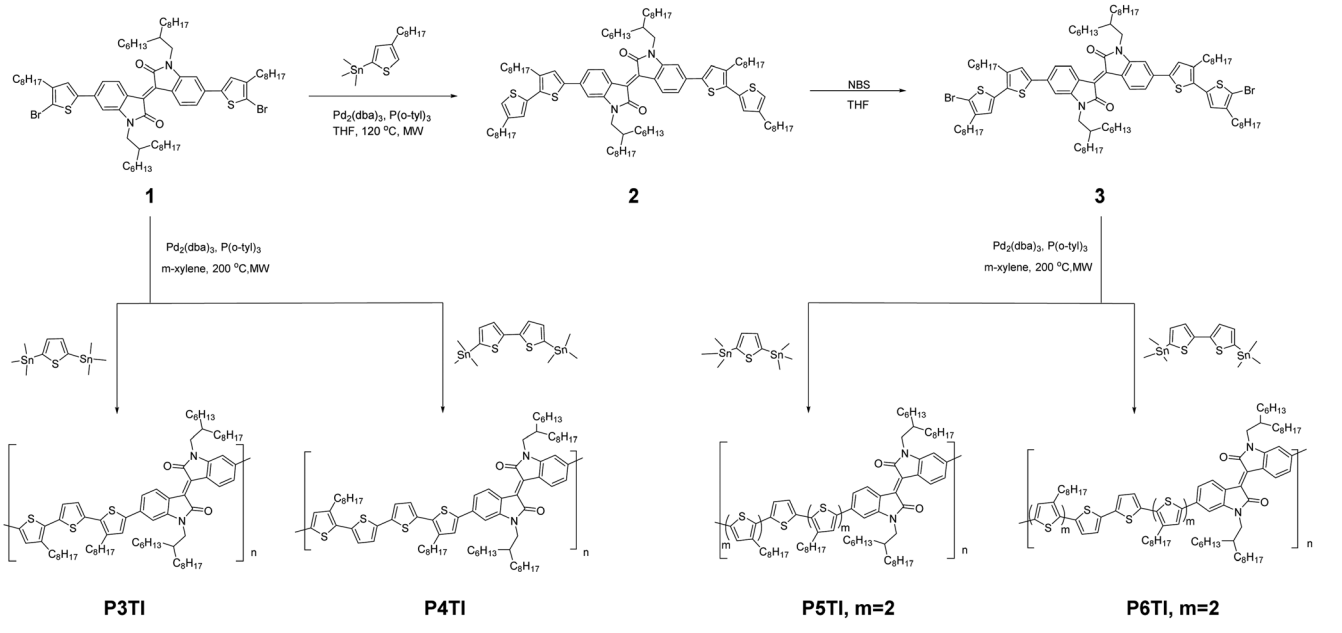

Scheme 1 Synthetic routes of P3TI, P4TI, P5TI and P6TI.

Table 1 Molecular properties and optical properties in chloroform and as-cast films of P*n*TIs

			Solution state			Solid state			
Polymer	M_n (kg mol^{-1})	PDI	$\lambda_1{}^a$ (nm)	$\lambda_2{}^b$ (nm)	$\lambda_3{}^c$ (nm)	$\lambda_1{}^a$ (nm)	$\lambda_2{}^b$ (nm)	$\lambda_3{}^c$ (nm)	E_g (eV)
P3TI	48	2.4	407	647	—	424	645	702	1.59
P4TI	26	2.1	444	638	687	450	645	706	1.58
P5TI	28	2.2	425	619	—	450	630	—	1.58
P6TI	35	1.8	444	619	—	468	630	—	1.57

^{a} π–π* transition. ^{b} Intramolecular charge transfer. ^{c} Intermolecular π–π interactions.

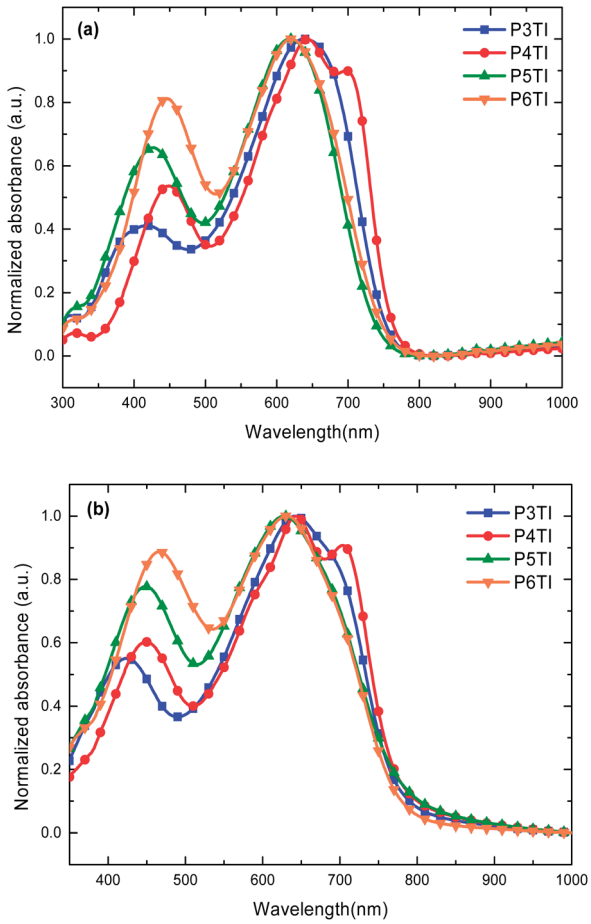

Fig. 1 UV-Vis absorption spectra of **P3TI**, **P4TI**, **P5TI**, and **P6TI** in chloroform solutions (a) and as-cast thin films (b).

which are related to intramolecular charge transfer (ICT) of polymers, are slightly blue-shifted with increasing the donor segment length. This shift results from the slightly diminished ICT effect between thiophene and isoindigo segments, suggesting that the electron-withdrawing effect of the isoindigo segments is reduced. However, the high-energy band of **P4TI** does not follow the same tendency; **P4TI** is more red-shifted compared to **P5TI**. This effect could be attributed to the fact that bithiophene in the donor segment has higher planarity than monothiophene. Moreover, an additional absorption band from intermolecular π–π interactions exists in the spectrum of **P4TI**, indicating that the polymers aggregate in the solution and thus confirming this polymer has poorer solubility compared to the others. For solid thin films, all absorption spectra are broader than those in the solution state, indicating that polymer aggregation and/or intermolecular π–π packing exists in the solid state. While the ICT bands of polymers are also slightly blue-shifted with increasing the donor segment length, the high-energy band of these polymers is red-shifted with the same trend, indicating that the donor segments in the main chains were reorganized in the solid state and became planer as compared to those in the solution state. All the polymers exhibit a low optical band gap (E_g) around 1.57–1.59 eV as determined from the onset of their absorption spectra, suggesting that these materials are good candidates for PSCs.

To investigate the influence of changing donor segments of the polymers on optoelectronic properties, cyclic voltammetry (CV) and density functional theory (DFT) simulation[37–39] were performed. Cyclic voltammograms of these polymers (Fig. S4†) only show reversible oxidation behavior, and their HOMO energy levels are deduced from the onset potentials. The HOMO energy levels of the polymers were calculated according to the following equation using ferrocene (Fc) as the internal standard: E_{HOMO} (eV) = $-(E_{onset,ox\ vs.\ Fe^+/Fe} + 5.13)$. Through subtraction from the optical band gap, the LUMO energy levels of the polymers were obtained and are listed in Table 2. The results indicate that the HOMO energy levels and the LUMO energy levels of these polymers are slightly increased when increasing the donor segment length. The upshifted HOMO energy levels are in agreement with the report from Yu's group showing that the HOMO energy level is primarily determined by the donor strength in a push–pull system;[9] the donor strength will be increased with increasing the thiophene number. Because the changes of energy levels are subtle, the HOMO energy levels, the LUMO energy levels, and the optical band gaps of these polymers remain around −5.37 to −5.49, −3.85 to

Table 2 Energy levels of P*n*TIs from cyclic voltammetry and DFT simulation

	CV		DFT calculation	
Polymer	HOMO (eV)	LUMO (eV)	HOMO (eV)	LUMO (eV)
P3TI	−5.49	−3.90	−5.06	−3.05
P4TI	−5.48	−3.90	−4.98	−3.06
P5TI	−5.44	−3.86	−4.89	−3.05
P6TI	−5.37	−3.80	−4.84	−3.07

−3.90, and 1.57–1.59 eV, respectively, and thus the optoelectronic properties of these polymers are still in the appropriate range for PCBM-based PSCs.[40] The DFT simulation was performed using Gaussian 09 with the B3LYP functional and the 6-31G* basis set. To reduce the computation time, two repeating units were used as a model for calculations. Note, the free chain ends could have dramatic influence on the internal dihedral angles of the polymer chains, thus resulting in the change of the electronic state and the band gap. Nevertheless, the results of DFT calculations (Table 2 and Fig. S5†) show similar trends of HOMO, LUMO, and band gap as observed experimentally.

Photovoltaic properties of the polymers were investigated by conventional solar cell configurations of ITO/PEDOT:PSS/polymer:$PC_{71}BM$/Ca/Al. The polymer:$PC_{71}BM$ weight ratios of 1 : 1, 1 : 1.5, and 1 : 2 and different combinations of processing solvents, dichlorobenzene (DCB), chlorobenzene (CB), DCB + CF (1 : 1 vol), DCB + 3 vol% diiodooctane (DIO), CB + 3 vol%, DCB + 3 vol% 1-chloronaphthalene (CN), and CB + 3 vol% CN were tested; every condition was tested with six separate devices (two 0.046 cm^2 active pixels per device). The optimized weight ratio for all polymers is 1 : 1.5, and the optimized processing solvents (for solubility) for **P3TI**, **P4TI**, **P5TI**, and **P6TI** are DCB + 3 vol% DIO, DCB + CF, DCB + 3 vol% DIO, and DCB + 3 vol% CN, respectively. The *J*–*V* curves of the optimized devices are shown in Fig. 2(a) and their photovoltaic characteristics are summarized in Table 3. Without additives, the short circuit current density (J_{sc}) of all polymers is low and the interfacial morphologies (not shown) measured by atomic force microscope (AFM) show large domains except for **P4TI**. With the assistance of additives, the J_{sc} and fill factor (FF) are enhanced for all the polymers and except for **P6TI** finer interfacial domain morphologies are observed (Fig. 3). For **P3TI**, a PCE of 6.36% (6.52% max.) with an open circuit voltage (V_{oc}) of 0.73 V, a J_{sc} of 13.78 mA cm^{-2}, and a FF of 0.65 was obtained. The result is close to that of Andersson's group and Wang's group under the same processing conditions showing that our material quality and device fabrication technique is comparable to theirs.[24,30] Although the V_{oc} of 0.76 V and a J_{sc} of 13.90 mA cm^{-2} of **P4TI** are higher than that of **P3TI**, the FF of 0.57 is smaller, and finally the PCE is only 5.83% (6.04% max.). The comparatively low efficiency could be attributed to the lack of uniformity in the active layer film caused by poor solubility even though the optimized processing solvent of DCB + CF for **P4TI** was used. For **P5TI**, a PCE of 3.65% (3.85% max.) with an open circuit voltage (V_{oc}) of 0.71 V, a J_{sc} of 8.83 mA cm^{-2}, and a FF of 0.62 was measured. Surprisingly, the J_{sc} is much lower than that of the others, and V_{oc} and FF remained comparable despite its broader UV-Vis absorption. A potential explanation for the low current is that the polymer does not have good crystallinity, thereby leading to lower hole mobility and thus lower J_{sc}. For **P6TI**, the highest PCE of 7.06% (7.25% max.) with a V_{oc} of 0.70, a J_{sc} of 16.24, and a FF of 0.64 was obtained. This polymer has broad UV-Vis absorption with good crystallinity (discussed in the next section) leading to the highest J_{sc}. However, the V_{oc} is slightly lower because its HOMO energy level is slightly higher than that of the others. To the best of our knowledge, this is the highest PCE and J_{sc} among the isoindigo-based polymers reported to date; this work highlights the great potential of simply adjusting chemical structures to achieve high-performance PSCs by simultaneously taking advantage of the broadened absorption spectrum and enhanced crystallinity, which combine to result in increased J_{sc}.

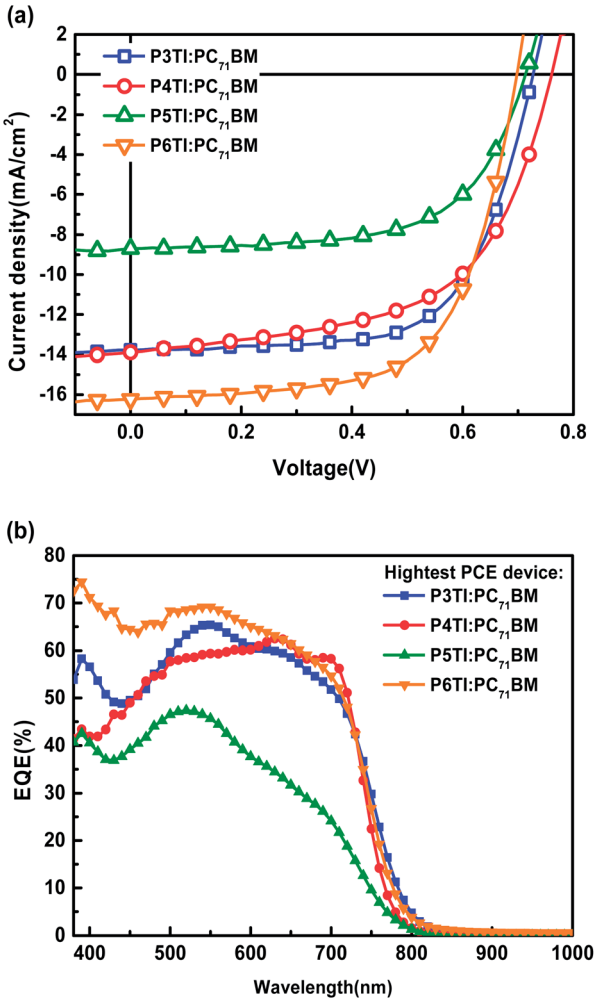

Fig. 2 (a) *J*–*V* curves and (b) EQE spectra of **P3TI**, **P4TI**, **P5TI**, and **P6TI** blended with $PC_{71}BM$ under their optimized conditions.

To check the accuracy of the obtained J_{sc}, the corresponding external quantum efficiencies (EQE) of the optimized solar cells were measured. In Fig. 2(b), the solar cells of all polymers exhibit a broad photoresponse from 350 to 800 nm. Except for **P5TI**, the EQE values of the polymers are over 50% in the range of 350–720 nm. The maximum EQE of the polymers is in the range of 450–600 nm which is consistent with their UV-Vis absorption spectra of the blend films (ESI, Fig. S6†). The calculated J_{sc} from integration of the EQE with an AM 1.5G reference spectrum is in agreement with J_{sc} determined from the *J*–*V* measurements (Table S1†).

In order to explore the correlation between chemical structures of the polymers and their resulting crystallinity, grazing incidence wide-angle X-ray scattering (GI-WAXS), and space charge limited current (SCLC) measurement of hole mobility were performed. As shown in Fig. 4, GI-WAXS studies revealed

Table 3 Characteristic properties of polymer solar cells and hole mobility of P*n*TI[a]

Polymer	V_{oc} (V)	J_{sc} (mA cm^{-2})	FF (%)	PCE avg. (%)	PCE max. (%)	μ_h (cm^2 V^{-1} s^{-1})
P3TI	0.73(±0.00)	13.80(±0.21)	63.61(±0.78)	6.39(±0.10)	6.52	3.68×10^{-5}
P4TI	0.76(±0.00)	13.51(±0.20)	57.86(±0.56)	5.96(±0.05)	6.04	3.17×10^{-4}
P5TI	0.72(±0.01)	8.28(±0.50)	61.75(±0.47)	3.65(±0.22)	3.85	2.80×10^{-5}
P6TI	0.71(±0.01)	15.74(±0.38)	63.90(±0.22)	7.10(±0.08)	7.25	8.93×10^{-5}

[a] Standard deviation of V_{oc}, J_{sc}, FF and PCE of the devices are presented in parentheses.

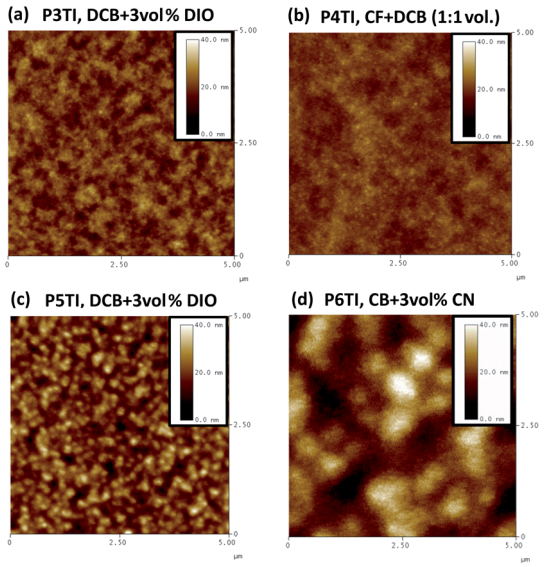

Fig. 3 AFM images of the active layers of polymer:$PC_{71}BM$ (1 : 1.5). (a) **P3TI** processed with DCB + 3 vol% DIO, (b) **P4TI** processed with CF + DCB (1 : 1 vol), (c) **P5TI** processed with DCB + 3 vol% DIO, and (d) **P6TI** processed with DCB + 3 vol% CN.

that all polymers have edge-on orientation wherein the π–π stacking direction is parallel to the substrate. The out-of-plane linecuts of GI-WAXS images (ESI, Fig. S7†) show that lamellar spacing of the polymers is in the range of 1.8–2.2 nm. Intensities of (100) reflections of the polymers are normalized with those of (200) reflections to estimate crystallinity of the polymers. Crystallinity follows the order: **P4TI** > **P6TI** > **P3TI** > **P5TI**. According to the previous work reported by Pei's group,[41] polymers with centrosymmetry have better crystallinity than those with axisymmetry, thus resulting in better charge mobility. This tendency provides an explanation for why **P4TI** and **P6TI**, where the thiophene numbers of the donor segment are even, have better crystallinity than the polymers with odd thiophene numbers (**P3TI** and **P5TI**). It is worth noting that the calculated ratio of the amount of thiophene with the side chain to the total amount of thiophene of **P3TI**, **P4TI**, **P5TI**, and **P6TI** is 0.67, 0.50, 0.80, and 0.67, respectively. The ratio not only has a roughly proportional correlation with the polymer solubility (higher ratio has better solubility) but also with the polymer crystallinity in the context of conformation asymmetry. Detailed studies of correlations between the chemical structures and solubility and crystallinity are ongoing. The results are also reflected in the hole mobility of the optimized polymer:PCBM blends, which

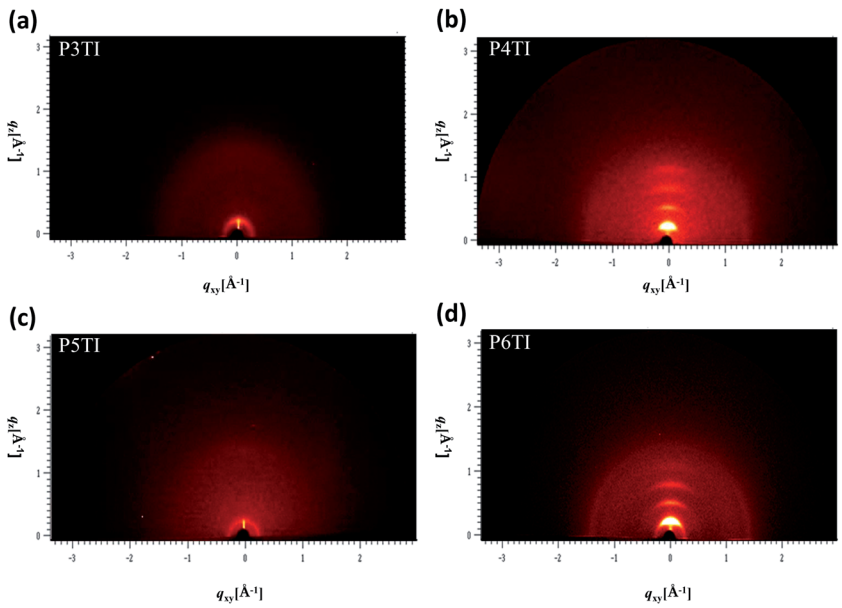

Fig. 4 Two-dimensional GIWAXS patterns of **P3TI** (a), **P4TI** (b), **P5TI** (c), and **P6TI** (d).

has been measured by the technique based on the SCLC model (see ESI†). The hole mobility is listed in Table 3 and found to be 3.68×10^{-5} cm^2 V^{-1} s^{-1} for **P3TI**, 3.17×10^{-4} cm^2 V^{-1} s^{-1} for **P4TI**, 2.80×10^{-5} cm^2 V^{-1} s^{-1} for **P5TI**, and 8.93×10^{-5} cm^2 V^{-1} s^{-1} for **P6TI**, respectively, which coincides with the GI-WAXS results. Higher hole mobility and suitable solubility of polymer will favor charge transport in photovoltaic devices and thus lead to better J_{sc} and device efficiency.

Conclusions

A series of isoindigo-based low-band-gap copolymers with an extended thiophene unit in the donor segment of the polymer were synthesized. The polymer absorption is broadened by increasing the length of the thiophene unit, while the HOMO and LUMO levels remain within an appropriate range for PCBM-based PSCs. As bithiophene was introduced in the donor segment with centrosymmetric conformation, the polymers indeed display better crystallinity and thus better hole mobility. Finally, with additional improved solubility, the polymer **P6TI** reaches the highest PCE of 7.25% (and a high J_{sc} of 16.24 mA cm^{-2}) among isoindigo-based low-band-gap copolymers to date. This work highlights that by simply adjusting the donor segment and implementing simple synthetic schemes, a material for high-performance and scalable PSCs will become available in the near future. Work targeting optimized chemical structure relevant to these polymers for reaching still higher efficiency is in progress.

Acknowledgements

We gratefully acknowledge the financial support from the National Science Council of Taiwan (NSC 99-2221-E-002-020-MY3, 101-2120-M-002-003, 101-3113-E-002-010, and 102-3113-P-002-027). We also thank the Department of Chemistry of National Taiwan University for use of their NMR spectrometer. Use of the Center for Nanoscale Materials at Argonne National Laboratory was supported by the US Department of Energy, Office of Science, Office of Basic Energy Sciences, under Contract no. DE-AC02-06CH11357.

Notes and references

1 J. W. Chen and Y. Cao, *Acc. Chem. Res.*, 2009, **42**, 1709–1718.
2 S. B. Darling and F. Q. You, *RSC Adv.*, 2013, **3**, 17633–17648.
3 G. Dennler, M. C. Scharber and C. J. Brabec, *Adv. Mater.*, 2009, **21**, 1323–1338.
4 C. Li, M. Y. Liu, N. G. Pschirer, M. Baumgarten and K. Mullen, *Chem. Rev.*, 2010, **110**, 6817–6855.
5 T. D. Nielsen, C. Cruickshank, S. Foged, J. Thorsen and F. C. Krebs, *Sol. Energy Mater. Sol. Cells*, 2010, **94**, 1553–1571.
6 C. J. Brabec, S. Gowrisanker, J. J. M. Halls, D. Laird, S. J. Jia and S. P. Williams, *Adv. Mater.*, 2010, **22**, 3839–3856.
7 Y. J. He, H. Y. Chen, J. H. Hou and Y. F. Li, *J. Am. Chem. Soc.*, 2010, **132**, 1377–1382.
8 Y. J. He, M. Shao, K. Xiao, S. C. Smith and K. L. Hong, *Sol. Energy Mater. Sol. Cells*, 2013, **118**, 171–178.
9 H. Zhou, L. Yang and W. You, *Macromolecules*, 2012, **45**, 607–632.
10 P. M. Beaujuge, C. M. Amb and J. R. Reynolds, *Acc. Chem. Res.*, 2010, **43**, 1396–1407.
11 P. L. T. Boudreault, A. Najari and M. Leclerc, *Chem. Mater.*, 2011, **23**, 456–469.
12 M. Jarosz, M. Puchalska, K. Polec-Pawlak, I. Zadrozna and H. Hryszko, *J. Mass Spectrom.*, 2004, **39**, 1441–1449.
13 M. J. Robb, S. Y. Ku, F. G. Brunetti and C. J. Hawker, *J. Polym. Sci., Part A: Polym. Chem.*, 2013, **51**, 1263–1271.
14 J. G. Mei, K. R. Graham, R. Stalder and J. R. Reynolds, *Org. Lett.*, 2010, **12**, 660–663.
15 R. Stalder, J. Mei and J. R. Reynolds, *Macromolecules*, 2010, **43**, 8348–8352.
16 Z. Ma, E. Wang, M. E. Jarvid, P. Henriksson, O. Inganas, F. Zhang and M. R. Andersson, *J. Mater. Chem.*, 2012, **22**, 2306–2314.
17 Z. F. Ma, E. G. Wang, K. Vandewal, M. R. Andersson and F. L. Zhang, *Appl. Phys. Lett.*, 2011, **99**, 143302.
18 R. Stalder, C. Grand, J. Subbiah, F. So and J. R. Reynolds, *Polym. Chem.*, 2012, **3**, 89–92.
19 E. Wang, Z. Ma, Z. Zhang, K. Vandewal, P. Henriksson, O. Inganäs, F. Zhang and M. R. Andersson, *J. Am. Chem. Soc.*, 2011, **133**, 14244–14247.
20 E. G. Wang, Z. F. Ma, Z. Zhang, P. Henriksson, O. Inganas, F. L. Zhang and M. R. Andersson, *Chem. Commun.*, 2011, **47**, 4908–4910.
21 G. Zhang, Y. Fu, Z. Xie and Q. Zhang, *Macromolecules*, 2011, **44**, 1414–1420.
22 Y. P. Zou, B. Liu, B. Peng, B. Zhao, K. L. Huang, Y. H. He and C. Y. Pan, *Polym. Chem.*, 2011, **2**, 1156–1162.
23 C. W. Wang, B. Zhao, Z. C. Cao, P. Shen, Z. Tan, X. L. Li and S. T. Tan, *Chem. Commun.*, 2013, **49**, 3857–3859.
24 E. G. Wang, Z. F. Ma, Z. Zhang, K. Vandewal, P. Henriksson, O. Inganas, F. L. Zhang and M. R. Andersson, *J. Am. Chem. Soc.*, 2011, **133**, 14244–14247.
25 K. Mahmood, Z. P. Liu, C. H. Li, Z. Lu, T. Fang, X. Liu, J. J. Zhou, T. Lei, J. Pei and Z. S. Bo, *Polym. Chem.*, 2013, **4**, 3563–3574.
26 M. Wan, H. Zhu, H. Deng, L. Jin, J. Guo and Y. Huang, *J. Polym. Sci., Part A: Polym. Chem.*, 2013, **51**, 3477–3485.
27 K. C. Cao, Z. W. Wu, S. G. Li, B. Q. Sun, G. B. Zhang and Q. Zhang, *J. Polym. Sci., Part A: Polym. Chem.*, 2013, **51**, 94–100.
28 T. Wang, Y. H. Chen, X. C. Bao, Z. K. Du, J. Guo, N. Wang, M. L. Sun and R. Q. Yang, *Dyes Pigm.*, 2013, **98**, 11–16.
29 M. Yang, X. W. Chen, Y. P. Zou, C. Y. Pan, B. Liu and H. Zhong, *J. Mater. Sci.*, 2013, **48**, 1014–1020.
30 Z. Ma, W. Sun, S. Himmelberger, K. Vandewal, Z. Tang, J. Bergqvist, A. Salleo, J. W. Andreasen, O. Inganas, M. R. Andersson, C. Muller, F. Zhang and E. Wang, *Energy Environ. Sci.*, 2014, **7**, 361–369.
31 E. H. Jung and W. H. Jo, *Energy Environ. Sci.*, 2013, **7**, 650–654.
32 C. C. Ho, S. Y. Chang, T. C. Huang, C. A. Chen, H. C. Liao, Y. F. Chen and W. F. Su, *Polym. Chem.*, 2013, **4**, 5351–5360.

33 T. Lei, Y. Cao, Y. Fan, C.-J. Liu, S.-C. Yuan and J. Pei, *J. Am. Chem. Soc.*, 2011, **133**, 6099–6101.
34 L. Biniek, S. Fall, C. L. Chochos, D. V. Anokhin, D. A. Ivanov, N. Leclerc, P. Leveque and T. Heiser, *Macromolecules*, 2010, **43**, 9779–9786.
35 M. P. Nikiforov, B. Lai, W. Chen, S. Chen, R. D. Schaller, J. Strzalka, J. Maser and S. B. Darling, *Energy Environ. Sci.*, 2013, **6**, 1513–1520.
36 T. Lei, Y. Cao, Y. L. Fan, C. J. Liu, S. C. Yuan and J. Pei, *J. Am. Chem. Soc.*, 2011, **133**, 6099–6101.
37 G. W. T. M. J. Frisch, H. B. Schlegel, G. E. Scuseria, M. A. Robb, J. R. Cheeseman, G. Scalmani, V. Barone, B. Mennucci, G. A. Petersson, H. Nakatsuji, M. Caricato, X. Li, H. P. Hratchian, A. F. Izmaylov, J. Bloino, G. Zheng, J. L. Sonnenberg, M. Hada, M. Ehara, K. Toyota, R. Fukuda, J. Hasegawa, M. Ishida, T. Nakajima, Y. Honda, O. Kitao, H. Nakai, T. Vreven, J. A. Montgomery Jr, J. E. Peralta, F. Ogliaro, M. Bearpark, J. J. Heyd, E. Brothers, K. N. Kudin, V. N. Staroverov, R. Kobayashi, J. Normand, K. Raghavachari, A. Rendell, J. C. Burant, S. S. Iyengar, J. Tomasi, M. Cossi, N. Rega, J. M. Millam, M. Klene, J. E. Knox, J. B. Cross, V. Bakken, C. Adamo, J. Jaramillo, R. Gomperts, R. E. Stratmann, O. Yazyev, A. J. Austin, R. Cammi, C. Pomelli, J. W. Ochterski, R. L. Martin, K. Morokuma, V. G. Zakrzewski, G. A. Voth, P. Salvador, J. J. Dannenberg, S. Dapprich, A. D. Daniels, Ö. Farkas, J. B. Foresman, J. V. Ortiz, J. Cioslowski and D. J. Fox, in *Gaussian 09, Revision A.1*, Gaussian, Inc., Wallingford, CT, 2009.
38 A. D. Becke, *J. Chem. Phys.*, 1993, **98**, 5648–5652.
39 C. T. Lee, W. T. Yang and R. G. Parr, *Phys. Rev. B: Condens. Matter Mater. Phys.*, 1988, **37**, 785–789.
40 M. C. Scharber, D. Muhlbacher, M. Koppe, P. Denk, C. Waldauf, A. J. Heeger and C. L. Brabec, *Adv. Mater.*, 2006, **18**, 789–794.
41 T. Lei, Y. Cao, X. Zhou, Y. Peng, J. Bian and J. Pei, *Chem. Mater.*, 2012, **24**, 1762–1770.